THRUST-TIME MEASUREMENTS OF SMALL SOLID PROPELLENT ROCKET MOTORS

By

Robert J. Beshara

Bachelor of Science

Oklahoma State University

Stillwater, Oklahoma

1958

Submitted to the Faculty of the Graduate School of
the Oklahoma State University
in partial fulfillment of the requirements
for the degree of
MASTER OF SCIENCE
May, 1961

THRUST-TIME MEASUREMENTS OF SMALL

SOLID PROPELLENT ROCKET MOTORS

Thesis Approved:

Paul A. McCollum

Thesis Advisor

Harold Fistor

Loren Mardesen

Dean of the Graduate School

PREFACE

There are vast amounts of instruments and transducers, which with proper use, can be employed to measure numerous and varied types of data. But no matter how much measuring equipment there is available, it is still required to use a good deal of ingenuity and design to make the more difficult measurements. The measurements spoken of here are "The Thrust-Time Measurements of Small Solid Propellent Rocket Motors."

Previous measurements of this type that have been noted by the writer have been inadequate, due to the fact that the thrust-time data of the rocket motor was superimposed on a decaying sinusoid. The decaying sinusoid being the characteristic of the thrust transducer and was initiated into oscillation by the initial shock of the rocket motor when fired. Needless to say that data extracted from these records would not be very reliable as far as maintaining a very high degree of accuracy.

This leads to the purpose of this paper, which is to provide a discussion of the design and techniques employed by the writer to set up an instrumentation system that is required to measure and record the thrust developed by small solid propellent rocket motors over the duration of their burning time. To achieve these results, the use of available commercial equipment along with original design will be employed.

The writer wishes to acknowledge Professor Paul A. McCollum for his astute advice and counseling throughout the preparation of this paper. To Douglas Aircraft Company, Inc., Tulsa, Oklahoma, I would like to express my thanks and appreciation for releasing much of the material used in this paper.

TABLE OF CONTENTS

LIST OF FIGURES

CHAPTER I

INTRODUCTION

A brief physical description and a few applications of the rocket motor are in order here to give a feel for what is to be measured and why.

The rocket motor and its major exterior dimensions are depicted in Figure 1.

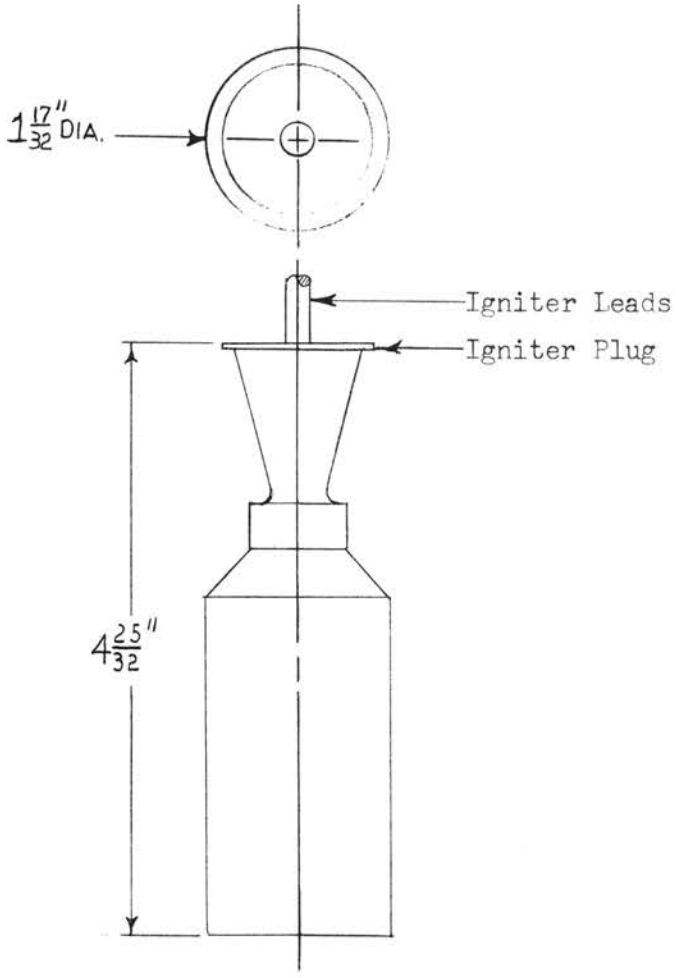

Figure 1. Top and Side View of the Rocket Motor.

The rocket motor is designed to develop approximately 40 pounds of thrust for one second, or a total impulse of 40 pound-seconds. The weight of the motor is approximately 0.6 pounds, and is fired by an electrical current applied to the igniter leads. The plug, which seats into the nozzle, contains the igniter and igniter leads, and it is blown free when the motor is fired.

These rocket motors were used to provide thrust for auxiliary spin and retro functions in a three stage missle space vehicle. The third stage-payload assembly and the various applications of the rocket motors are shown in Figure 2.

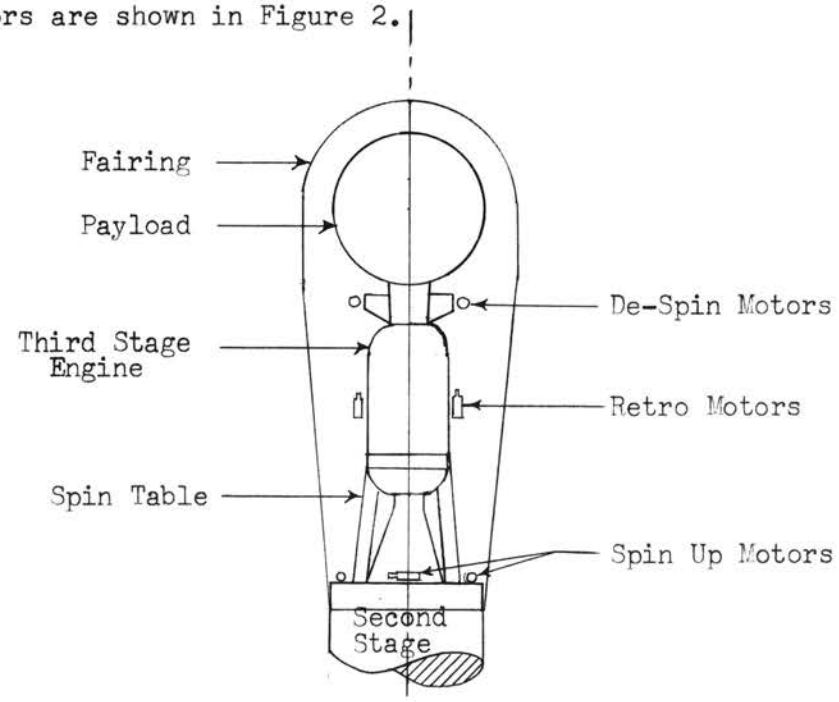

Figure 2. Third Stage-Payload Assembly.

The third stage-payload assembly is mounted on a spin table attached to the second stage. The spin-up motors are fired a short time prior to third and second stage separation and the thrust of these motors spins up the third stage-payload assembly to a desired RPM. This is done to stabilize the third stage-payload assembly

during the remainder of its flight. When the third stage engine has placed the payload in its prescribed orbit, the third stage engine is separated from the payload and the retro rocket motors are fired to push the third stage engine away from the payload. The de-spin rocket motors are fired a short time later to bring the payload to a no spin condition.

It can be seen from the above discussion that accurate thrust-time or impulse data of these rocket motors is very important to the success of the sequence of events that occur in the third stage-payload assembly.

There are four major factors to consider in an instrumentation system that will obtain thrust-time data for small solid propellent rocket motors. These are listed below.

1) Detecting the desired data from the rocket motors.
2) Converting this data from a mechanical to an electrical quantity.
3) Amplification of this electrical signal.
4) Recording the data against time.

The requirements of these four factors are governed by the system specifications, which are listed below.

1) Range: 0 to 100 pounds.
2) Rise time: 0 to steady state in not more than 4 milliseconds with a step input.
3) Overshoot: To be not more than 1% above steady state with a step input.
4) Paper speed of the recorder: To be not less than 100 inches per second.

It might be noted here concerning the second and third specifications, that the design calculations was to be carried out as close to these figures as possible. This would help offset any fabricating tolerances incurred during the construction of the instrumentation system. After a system is constructed, it is unlikely that it will perform to exact specifications, but final adjustments can be made to achieve the desired performance.

Since the success of the instrumentation system is dependent mainly on the system specifications and meeting these specifications, a discussion of each will follow.

Although the thrust of the rocket motors is approximately 40 pounds, the range of 0 to 100 pounds was selected because it is anticipated that the rocket motors will give a surge thrust when the igniter plug is blown free of the motor. The magnitude of this surge is governed in part by how tight the igniter plug is seated in the nozzle.

The rise time of 0 to steady state in not more than 4 milliseconds with a step input was choosen since it is anticipated that the rocket motor will have a rise time somewhat more than this.

Holding the overshoot to 1% or less will permit only a minimum amount of oscillation from the instrumentation system to appear in the data.

The paper speed of 100 inches per second was specified to get a clear indication of the rocket motor rise time, overshoot and any other phenomena that might occur during the burning time of the rocket motor.

The four major factors discussed previously will be satisfied

by the items listed below.

1) Thrust transducer with a strain gage bridge read out.

2) Carrier amplifier.

3) High speed recording oscillograph in conjunction with a high frequency galvonometer.

The remainder of this paper will be devoted to developing the instrumentation system into a compatible unit that meets the specifications.

CHAPTER II

DESIGN OF THE THRUST TRANSDUCER

As shown in Figure 3, a deflecting cantilever beam with damping, and employing a strain gage bridge read out, will be the principle used in the design of the thrust transducer.

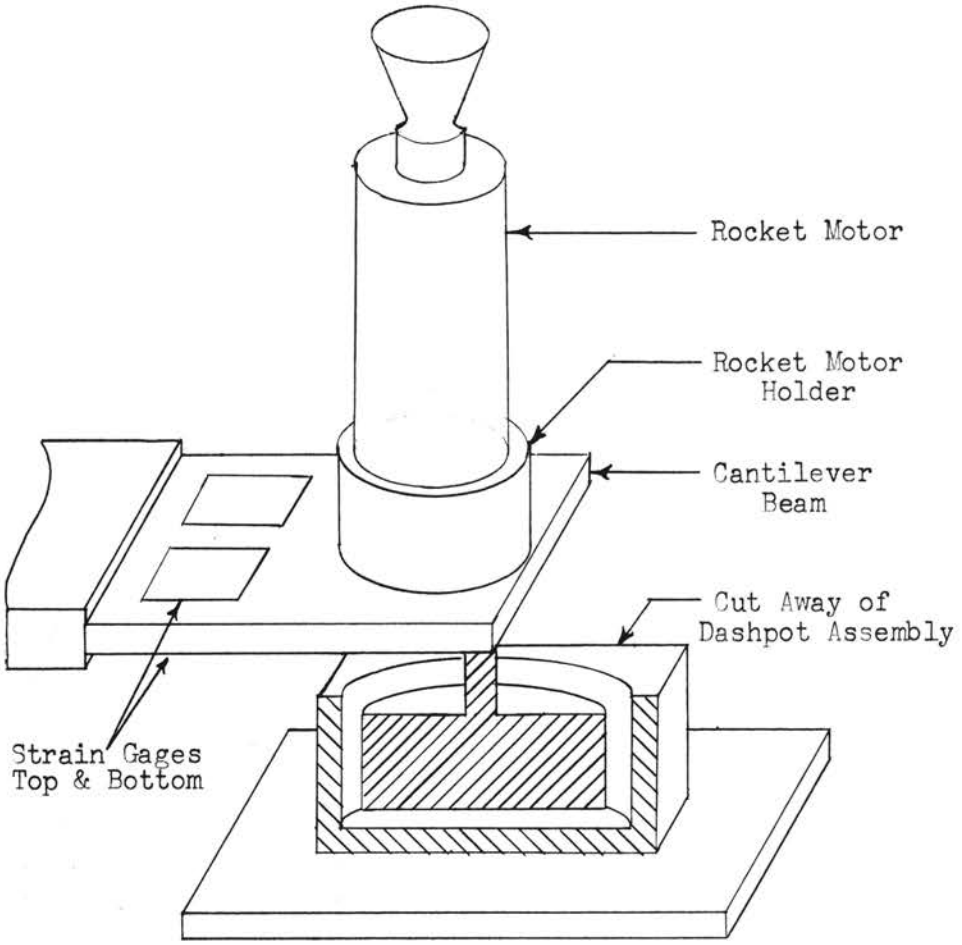

Figure 3. Sketch of the Thrust Transducer.

The transducer will operate in this manner: When the rocket motor is fired, the beam will deflect an amount proportional to the thrust of the rocket motor. The deflection of the beam will stretch the top pair of strain gages and compress the bottom pair, thereby increasing the resistance of the top pair and decreasing the resistance of the bottom pair. The gages will be wired as an additive bridge network. The dashpot serves the purpose of suppressing any oscillation when the motors are fired.

As can be seen from Figure 3, the transducer resolves into a spring-mass-damped system. The spring being the cantilever beam, the mass being the entire weight supported by the beam, and the damper being the dashpot assembly. It is assumed that the transducer will be operated in its linear range.

The design of the transducer will be divided into four parts. These are listed below.

1) Determining ω_n, the undamped natural angular frequency of the transducer, and ζ the damping factor of the transducer to satisfy specifications two and three.
2) The design of the rocket motor holder and the dashpot piston; and a weight estimate of all moving members of the transducer.
3) The design of the cantilever beam.
4) The design of the dashpot assembly.

Determining ω_n and ζ .

An equivalent sketch of the transducer is shown in Figure 4, from which the force balance differential equation is written with the transducer in the equilibrium position.

$$T(t) = M\frac{d^2x}{dt^2} + C\frac{dx}{dt} + Kx, \qquad (1)$$

where $T(t)$ is a step input. With the initial velocity $v(0)=0$ and the initial displacement $x(0)=0$, the Laplace transformation[1] of (1) is

$$X = \frac{T}{S} \frac{1}{MS^2+CS+K} \quad , \qquad (2)$$

where $S=\sigma+j\omega$, a complex variable.

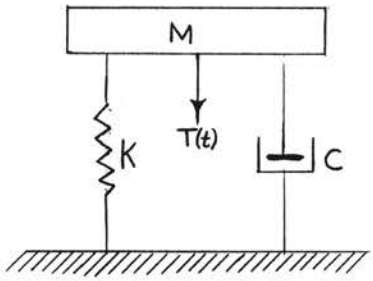

Figure 4. Equivalent Sketch of the Transducer.

To illustrate the transducer characteristics as M, C and K are varied, a root locus plot[2] will be made as each respectively, is varied from 0 to ∞.

From Figure 5 it can be seen that, when the locus lies in the second and third quadrant, the transducer is oscillatory or underdamped. When the locus lies at the saddle points, the transducer is critically damped and when the locus lies on the negative real axis, other than the saddle points, the transducer is overdamped.

From the foregoing observations it can be concluded that there are three possible solutions to the differential equation (1). They are:

1) The underdamped case - - - - - $C^2/4M^2 < K/M$

2) The critically damped case - - $C^2/4M^2 = K/M$

3) The overdamped case - - - - - $C^2/4M^2 > K/M$

Since the design is to be carried out with a small amount of overshoot, the solution of the underdamped case is the one needed.

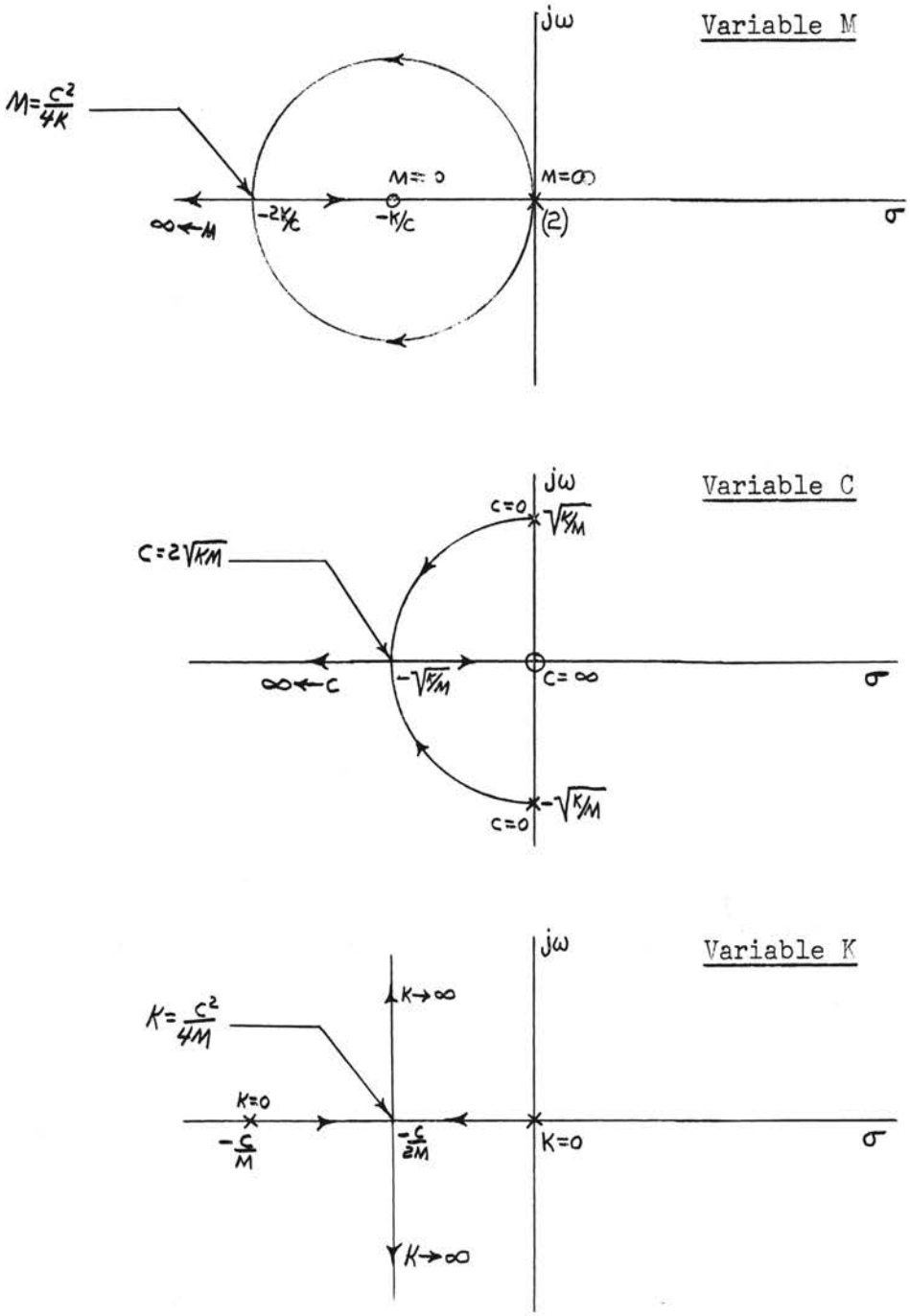

Figure 5. Root Locus Plot as M, C and K are Varied From 0 to ∞ .

Now the transducer weighting function[3] will be found from the differential equation (1) for the underdamped case with the thrust input equal to a unit impulse. From this, (2) becomes

$$\chi(s) = \frac{1}{Ms^2 + cs + K} \,, \tag{3}$$

and the inverse transform of (3) is

$$\chi(t) = W(t) = \frac{1}{M} \frac{\epsilon^{-c/2M\,t}}{\sqrt{K/M - c^2/4M^2}} \sin \sqrt{K/M - c^2/4M^2}\; t \,, \tag{4}$$

where $W(t)$ is the transducer weighting function.

With the transducer weighting function known, the convolution integral[1] will now be employed to determine the response of the transducer to a step input of thrust. The convolution integral is

$$\chi(t) = \int_0^t f_1(t-\gamma)\, f_2(\gamma)\, d\gamma \,, \tag{5}$$

where γ is a time shift variable, $f_1(t-\gamma) = T\mu(t-\gamma)$ and $f_2(\gamma) = W(\gamma)$. Inserting these functions into (5), the expression

$$\chi(t) = \int_0^t T\mu(t-\gamma) \frac{1}{M} \frac{\epsilon^{-c/2M\,t}}{\sqrt{K/M - c^2/4M^2}} \sin \sqrt{K/M - c^2/4M^2}\; \gamma \, d\gamma \tag{6}$$

is obtained. Since $\mu(t-\gamma)$ equals unity for $t > \gamma$ and zero for $t < \gamma$, (6) becomes

$$\chi(t) = \frac{T}{M\sqrt{K/M - c^2/4M^2}} \int_0^t \epsilon^{-c/2M\,\gamma} \sin \sqrt{K/M - c^2/4M^2}\; \gamma \, d\gamma \,. \tag{7}$$

Upon integrating (7) between the limits of 0 to t, the response of the transducer with a step input of thrust is found to be

$$\chi(t) = T/K \left\{ 1 - \frac{\sqrt{K/M}}{\sqrt{K/M - c^2/4M^2}}\, \epsilon^{-c/2M\,t} \sin\left(\sqrt{K/M - c^2/4M^2}\; t + \psi\right) \right\} \,, \tag{8}$$

where $\psi = \arctan\left\{ \sqrt{K/M - c^2/4M^2} \Big/ c/2M \right\}$.

Since the specifications are given indirectly in terms of the

natural angular frequency (ω_n) and the damping (ζ), it is desired to write (8) in terms of ω_n and ζ instead of M, C, and K.

It can be seen from (8) that $\sqrt{K/M - C^2/4M^2}$ is the damped natural angular frequency of the transducer. Also, if $C = 0$ (no damping), the natural angular frequency of the transducer is

$$\omega_n = \sqrt{K/M} \,. \tag{9}$$

Factoring $\sqrt{K/M}$ from $\sqrt{K/M - C^2/4M^2}$ yields

$$\sqrt{K/M}\,\sqrt{1 - C^2/4KM} = \omega_n \sqrt{1-\zeta^2}\,, \tag{10}$$

where

$$\zeta = C/2\sqrt{KM} \,. \tag{11}$$

Writing (8) in terms of (9), (10), and (11) yields

$$x(t) = T/K\left\{1 - \frac{\epsilon^{-\zeta\omega_n t}}{\sqrt{1-\zeta^2}} \sin(\omega_n\sqrt{1-\zeta^2}\,t + \psi)\right\}, \tag{12}$$

where $\psi = \arctan\left\{\sqrt{1-\zeta^2}/\zeta\right\}$. (13)

ω_n and ζ must be found to satisfy the specifications, bearing in mind that x(t) must go from zero to steady state (x_{ss}) in not more than 4 milliseconds and the overshoot is to be not more than 1%.

By differentiating (12) with respect to time and setting this equal to zero, the time at which the maximum and minimum points of x(t) occur may be found.[4] Hence,

$$\frac{dx}{dt} = T/K\left\{\frac{\zeta\omega_n \epsilon^{-\zeta\omega_n t}}{\sqrt{1-\zeta^2}} \sin(\omega_n\sqrt{1-\zeta^2}\,t + \psi) - \omega_n \epsilon^{-\zeta\omega_n t} \cos(\omega_n\sqrt{1-\zeta^2}\,t + \psi)\right\} = 0, \tag{14}$$

or

$$\tan(\omega_n\sqrt{1-\zeta^2}\,t + \psi) = \sqrt{1-\zeta^2}/\zeta \,. \tag{15}$$

Employing the double angle trigonometric identity,[5] (15) may be written as

$$\frac{\tan(\omega_n\sqrt{1-\zeta^2})t + \tan\psi}{1-\tan(\omega_n\sqrt{1-\zeta^2})t\tan\psi} = \sqrt{1-\zeta^2}/\zeta . \qquad (16)$$

From (13), $\tan\psi = \sqrt{1-\zeta^2}/\zeta$, therefore

$$\tan(\omega_n\sqrt{1-\zeta^2})t = 0. \qquad (17)$$

(17) is equal to zero when $\omega_n\sqrt{1-\zeta^2}t = 0, \pi, 2\pi, 3\pi, \ldots\ldots\ldots$ The minimum values of $x(t)$ occur when $\omega_n\sqrt{1-\zeta^2}t = 0, 2\pi, \ldots\ldots$, and the maximum values of $x(t)$ occur when $\omega_n\sqrt{1-\zeta^2}t = \pi, 3\pi, \ldots\ldots\ldots$ That is to say, the damped sine term in (12) alternates above and below the steady state value of $x(t)$ every π radians. The maximum overshoot will occur when the step input is initially applied. Therefore,

$$\omega_n\sqrt{1-\zeta^2}t = \pi \qquad (18)$$

at the maximum value of $x(t)$.

Since there are two unknowns (ω_n and ζ), and only one equation (18), another equation is required to find ω_n and ζ to satisfy the specifications. The second equation will be derived from (12).

Noting (12), it can be seen that as $t \to \infty$, $x(t) \to T/K$ which is the steady state solution of $x(t)$ (x_{ss}), and the term containing the damped sine expression is the transient solution of $x(t)$(x_t). Overshoot is defined as the ratio of δ/x_{ss}, where δ is the maximum diviation of $x(t)$ above x_{ss}, and as stated in (18) the maximum overshoot will occur at $\omega_n\sqrt{1-\zeta^2}t = \pi$.

From the foregoing discussion, (12) may now be written as

$$x_{ss} + \delta = x_{ss}\left\{1 - \frac{e^{-\pi\zeta/\sqrt{1-\zeta^2}}}{\sqrt{1-\zeta^2}}\sin(\pi+\psi)\right\}, \qquad (19)$$

or

$$\delta/x_{ss} = \frac{\epsilon^{-\pi\zeta/\sqrt{1-\zeta^2}}}{\sqrt{1-\zeta^2}} \sin\psi \,. \tag{20}$$

By (13), $\sin\psi = \sqrt{1-\zeta^2}$, thus (20) becomes

$$\delta/x_{ss} = \epsilon^{-\pi\zeta/\sqrt{1-\zeta^2}} \,, \tag{21}$$

or

$$\zeta = \ln\left(x_{ss}/\delta\right) \Big/ \sqrt{\pi^2 + \left[\ln\left(x_{ss}/\delta\right)\right]^2} \,. \tag{22}$$

Since δ/x_{ss} is known to be 0.01 from the specifications, ζ may now be evaluated. Thus,

$$\zeta = 0.82 \tag{23}$$

To evaluate ω_n , it is recalled that when $x(t) = x_{ss}$

$$\sin(\omega_n\sqrt{1-\zeta^2}\,t + \psi) = 0 \,, \tag{24}$$

or

$$\tan(\omega_n\sqrt{1-\zeta^2}\,t) = -\tan\psi = \tan(-\psi) \,, \tag{25}$$

and by (13) and (23) $$\psi = 35^\circ. \tag{26}$$

$(-\tan\psi)$ will occur only in the second and fourth quadrant. $(-\tan\psi)$ will be in the second quadrant when $x(t)$ starts to go above x_{ss} and in the fourth quadrant when $x(t)$ returns to x_{ss}. The first case is the one of interest, thus

$$\omega_n\sqrt{1-\zeta^2}\,t = 180^\circ - 35^\circ = 2.53 \text{ radians.} \tag{27}$$

From the specifications t is known to be 4 milliseconds and from (23), $\zeta = 0.82$, thus

$$\omega_n \geq 1100 \text{ radians/second.} \tag{28}$$

To insure a rise time of not more than 4 milliseconds, ω_n will be increased to $$\omega_n = 1200 \text{ radians/second.} \tag{29}$$

Weight Estimate.

It can be seen from (9) and (11) that the mass of the transducer moving parts must be known to determine K, the stiffness of the beam, and C, the viscous damping of the transducer.

The rocket motor weight is known from the manufacturer's data. The basic dimensions of the rocket motor holder and dashpot piston will now be designed to determine their weights. The weight of the cantilever beam will be estimated.

The rocket holder is shown in Figure 6.

Material:
Steel

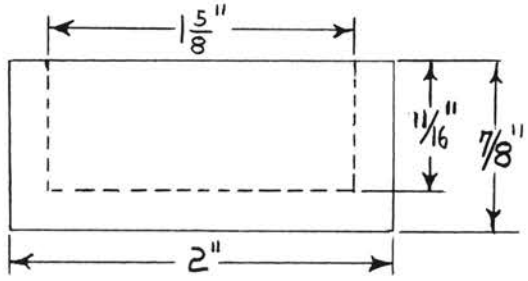

Figure 6. Rocket Motor Holder.

The dashpot piston is shown in Figure 7.

Material:
Aluminum

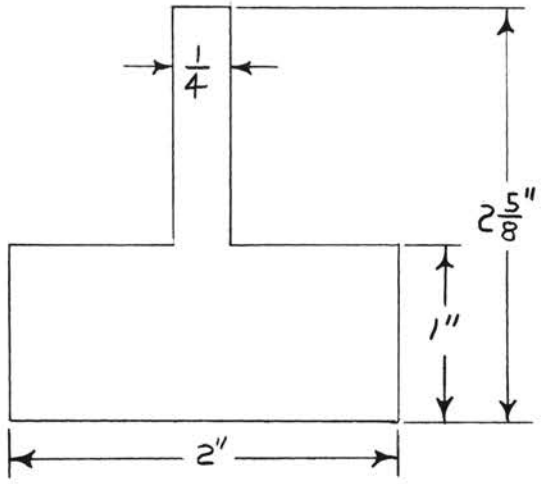

Figure 7. Dashpot Piston.

The cantilever beam is shown in Figure 8.

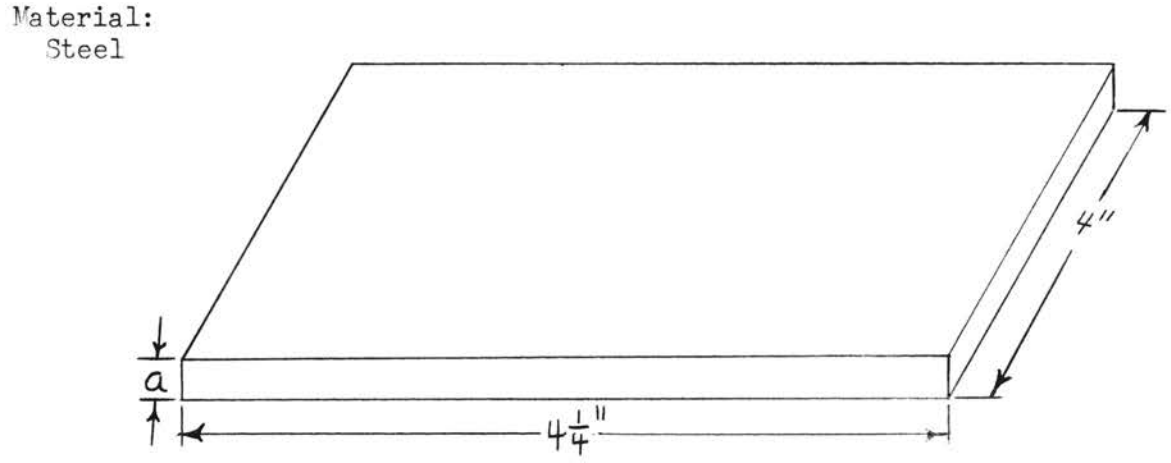

Figure 8. Cantilever Beam.

The length of 4 1/4" and the width of 4" are selected to allow adequate space for the location of the rocket motor holder and the strain gages. The thickness of the beam (a) will be calculated to achieve the desired natural frequency.

Summation of the weight estimates.

1) Rocket motor = 0.6 pounds.

2) Rocket motor holder = 0.3 pounds.

3) Dashpot piston and assorted hardware = 0.3 pounds.

4) Cantilever beam = 1.2 pounds.

Total weight estimate = 2.5 pounds.

Design of the Cantilever Beam.

Since ω_n and M are now known, K may be calculated by (13) and the thickness of the beam (a) can be determined. So by (13)

$$K = 9330 \text{ pounds/inch.} \tag{30}$$

The deflection formula[6] for cantilever beams will be employed to find the stiffness (a).

$$K = \frac{6EI}{\ell^2(3L - \ell)} \tag{31}$$

where E is the modulus of elasticity of steel -30 X 10^6 psi , I is the moment of inertia of the beam about the width axis - $\frac{Wa^3}{12}$, L is the length of the beam -4.25 inches, and ℓ is the length from the base of the beam to where the load is applied -3.25 inches. Inserting these values and (30) into (31) yields

$$a^3 = 0.0156 \text{ cubic inches,} \tag{32}$$

or

$$a = 0.25 \text{ inches.} \tag{33}$$

From (33) it is concluded that the beam be 0.25 inches thick for the transducer to have a natural angular frequency of 1200 radians/second.

Design of the Dashpot.

Since ζ , M and K are known, the damping coefficient (C) may be calculated. By (11),

$$C = 2\zeta\sqrt{KM} ,$$

or

$$C = 12.7 \text{ pounds/in/sec.} \tag{34}$$

In this design, a viscous fluid for the dashpot assembly will be selected. The clearance gap between the piston and cylinder walls will be treated as a circular pipe and the pipe diameter will be calculated to achieve the proper damping.

The empirical formula for laminar flow[7]

$$\Delta p/_{\ell} = \frac{k\mu Q}{d^4} \tag{35}$$

will be employed to calculate the pipe diameter (d), and k is a proportionality constant and equal to 0.000273, Q is the flow in gallons per minute, μ is the viscoscity of the fluid in centipoise, and $\Delta p/_{\ell}$ is the pressure drop per unit length in psi per foot.

The fluid selected for this calculation was SAE 30 lubricating oil. This fluid has a viscoscity of approximately 500 centipoise at 70° F.

The average velocity of the piston is approximately

$$V = \frac{\Delta x}{\Delta t} = \frac{x_{ss}}{\text{RISE TIME}} \quad (36)$$

or

$$V = 1.07 \text{ in/sec.} \quad (37)$$

The force applied to the cross sectional area of fluid under the piston is

$$F = CV = (12.7)(1.07) = 13.6 \text{ pounds,} \quad (38)$$

and the cross sectional area is

$$A = \frac{\pi D^2}{4} = \pi \text{ sq. in.} \quad (39)$$

Dividing (38) by (39) and the length of the piston (1/12 ft.) yields the pressure drop per unit length required to give the proper damping. Hence,

$$\Delta P/_y = \frac{(13.6)(12)}{3.1416} = 52.0 \text{ PSI/Ft.} \quad (40)$$

The rate of flow in gallons per minute is given by

$$Q = F/A(V) = \frac{(13.6)(1.07)(60)}{(3.1416)(231)} = 1.2 \text{ GPM.} \quad (41)$$

Inserting k, μ, (40) and (41) into (35) yields

$$d^4 = \frac{(0.000273)(500)(1.2)}{52} = 0.00315 \text{ IN}^4, \quad (42)$$

or

$$d = 0.135 \text{ inches.}$$

The area of the clearance between the piston and cylinder wall is

$$\frac{\pi d^2}{4} = \frac{\pi D_2^2}{4} - \frac{\pi D^2}{4}, \quad (43)$$

where D_2 is the diameter of the cylinder. Solving (43) for D_2 yields

$$D_2 = \left\{2^2 + (.135)^2\right\},$$

or

$$D_2 = 2.01 \text{ inches.} \tag{44}$$

The clearance is given by

$$C_G = \frac{D_2 - D_1}{2} = 5/1000 \text{ inch.} \tag{45}$$

A clearance this small between the piston and cylinder wall would not leave much room for machining tolerances. So to relieve this problem somewhat, the clearance gap was increased to equal

$$C_G = 10/1000 \text{ inch.} \tag{46}$$

The design of the dashpot was carried out to obtain a reasonable figure for the clearance between the piston and cylinder wall. It is very unlikely that the transducer will have exactly a damping factor of 0.82 with the fluid selected initially. This can be contributed to the increase in gap clearance, machining tolerances in the fabrication of the cylinder and piston, the vicoscity of the fluid not being the value read off the manufacturer's graph sheet, and the design by empirical formula. However, this may be remedied after the transducer is fabricated and assembled. If the transducer doesn't perform satisfactorily with the original fluid selected, there is a wide variety of inexpensive lubricating oils of various weights and viscosities that can be tried until the proper damping is achieved. In the final adjustments, the writer tried three different weights of lubricating oil and a MIL O-560S hydraulic oil, the latter being the fluid that gave the transducer the proper damping.

The transducer design is now complete, except for assemblage hardware, which was omitted because it would not contribute to the purpose of this paper.

CHAPTER III

STRAIN GAGE BRIDGE, CARRIER AMPLIFIER, GALVONOMETER AND OSCILLOGRAPH CONSIDERATIONS.

As suggested by its name, the strain gage operates on the principle of strain. This is, a given strain will cause an elongation of the gage which thereby causes a change in its resistance. The strain gage is a bilateral device which can be used in compression of tension.

For this application, a four active arm bridge will be used, two in compression and two in tension. There are two major advantages in using a four active arm bridge over a single active arm bridge. These are: four times more sensitivity than a single active arm bridge, and self temperature compensating.

An analysis of the strain gage bridge with a carrier excitation will now be made, bearing in mind that the strain and change in resistance of the bridge is directly proportional to the deflection $x(t)$ of the transducer and thereby the thrust of the rocket motor.

The circuit diagram for the strain gage bridge and the carrier excitation is shown in Figure 9.

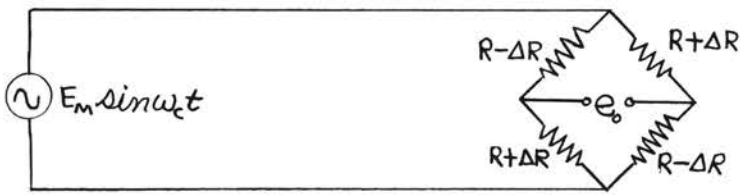

Figure 9. Strain Gage Bridge and Carrier Excitation Diagram.

From Figure 9, E_M is the carrier voltage, ω_c is the carrier angular frequency, R is the nominal gage resistance, ΔR is an increase in resistance of the gage due to tension, $-\Delta R$ is a decrease in resistance of the gage due to compression and e_o is the resultant output voltage due to an unbalance in the bridge.

Assume at present that the carrier excitation voltage is direct rather than alternating and that ΔR varies sinusoidally at an angular frequency ω_m.

The output voltage equation in terms of excitation and the circuit resistances is

$$e_o = \frac{E_M(R+\Delta R \sin \omega_m t)}{R+\Delta R \sin \omega_m t + R - \Delta R \sin \omega_m t} - \frac{E_M(R-\Delta R \sin \omega_m t)}{R+\Delta R \sin \omega_m t + R - \Delta R \sin \omega_m t} \quad (1)$$

where ω_m is the modulating angular frequency. Upon simplifying, (1) becomes

$$e_o = \frac{E_M \Delta R}{R} \sin \omega_m t \quad (2)$$

Substituting $E_M \sin \omega_c t$ for E_M, yields

$$e_o = \frac{E_M \Delta R}{R} \sin \omega_c t \sin \omega_m t, \quad (3)$$

or

$$e_o = \frac{E_M \Delta R}{R} \left\{ \cos(\omega_c + \omega_m)t - \cos(\omega_c - \omega_m)t \right\}. \quad (4)$$

From (4) it is seen that a double sideband suppressed carrier signal is present at the output. Therefore, along with amplification, the output must be detected with a phase sensitive detector which supplies the missing carrier. Once this is accomplished the output may be plotted on a recording oscillograph. The carrier amplifier frequency must be about 7 times greater than the modulating frequency.

The carrier amplifier selected for this instrumentation system

has a carrier frequency of 20 kilocycles, at a maximum excitation voltage of 5 volts RMS, a useful frequency range of 0 to 3000 cycles per second and a maximum gain of 1000.

As stated in the system specifications, the paper speed of the recording oscillograph must be at least 100 inches per second. There are a good many oscillographs on the market that can attain this recording speed and much more. The instrument selected for this system was a Century 408 recording oscillograph.

The galvonometer selected to be used in conjunction with the oscillograph was the Century 210C53-3 galvonometer. The Century 210C53-3 galvonometer was selected because of its high natural frequency as compared to the transducer natural frequency. It characteristics are:

1) Natural frequency - 850 cps.

2) Resistance of the coil - 40 ohms.

3) Damping - 64%.

4) DC sensitivity - 3.23 milliamps per inch.

CHAPTER IV

CHECK OUT AND CALIBRATION

After the complete assembly of a designed system it is desirable to check the system out throughly before putting it to use for the purpose for which it is intended.

Since the clearance between the piston and cylinder wall of the dashpot assembly was very small, 0.001 inches, it is likely that the piston will touch the cylinder wall with or without a load on the transducer. If the piston were allowed to touch or rub the cylinder wall, the data obtained from the system would be worthless because the friction between the piston and cylinder wall would restrain the cantilever beam from making a true deflection.

The alignment of the piston and cylinder was achieved by mounting the dashpot cylinder and pedestal on an insulating board. An ohmmeter was then used to check continuity between the piston and cylinder wall. The cylinder was adjusted until the ohmmeter read open circuit with the cantilever beam loaded and unloaded. Thus, the piston was properly aligned.

Next, it was desired to determine if the fluid selected for the dashpot would give the transducer the proper damping.

This check out was done by giving the transducer an initial displacement input and recording the transient response of the transducer. If the transducer response was overdamped, a lighter or less

viscous fluid could be tried, of if the response was underdamped or highly oscillatory, a heavier or more viscous fluid could be tried. This procedure could be followed until the proper response was obtained.

The calibration of the system was a simple matter. A known dead weight was placed on the transducer with its center of gravity placed directly in line with the center line of the rocket motor thrust vector. The deflection of the galvonometer was noted and tabulated. This procedure continued with different weights until the system was calibrated from 0 to 100 pounds.

CHAPTER V

SUMMARY

In Chapter I, the need for improved thrust-time measurements was established by a discussion of previous measurements of this type and by the critical application of the rocket motor in the missle field. Also, the requirements of the instrumentation system were specified and discussed to provide an insight to the problem at hand.

Chapter II provided a discussion of a design of a thrust transducer. This included: selecting the principle of a damped deflecting cantilever beam for the transducer and resolving it into a second order linear differential equation; investigating the three possible solutions of the differential equation by the root locus plot shown in Figure 5; determining the transducer weighting function and using it in conjunction with the convolution integral to find the response of the system to a step input; the derivation of two equations from the solution of the differential equation and the system specifications to find the required natural angular frequency and the damping factor of the transducer; estimating the mass of the transducer moving parts; and the design of the cantilever beam and dashpot assembly.

A circuit analysis of the strain gage bridge excited by a carrier voltage was presented in Chapter III. The analysis show that,

along with amplification, the output of the bridge must be detected by a phase sensitive detector which supplies the missing carrier. Also included in Chapter III was the selection of the recording oscillograph and associated galvonometer.

Chapter IV provided a discussion of the techniques used in checking out the instrumentation system so as to remedy any faults the system might have. Also, the calibration procedure of the system was presented.

The completed instrumentation system to measure thrust-time data of small solid propellent rocket motors performed satisfactorily in all aspects. The data records were essentially "clean," that is to say, there was a minimum amount of noise appearing in the data. Because of this, extracting the data from the records was a fairly easy process. The system provided reliable data with a good degree of accuracy and after many thrust-time measurements, the instrumentation system still performed satisfactorily.

BIBLIOGRAPHY

1. Gardner, Murray F., and Barnes, John L., Transients in Linear Systems, Vol. I, New York: John Wiley and Sons, Inc., 1958.

2. Chestnut, Harold, and Mayer, Robert W., Servomechanisms and Regulating System Design, Vol. I, 2nd Ed., New York: John Wiley and Sons, Inc., 1959.

3. Goldman, Stanford, Transformation Calculus and Electrical Transients, Englewood Cliffs, N. J.: Prentice-Hall, Inc., 1958.

4. Smail, Lloyd L., Calculus, New York: Appleton-Century-Crofts, Inc., 1949.

5. Burington, Richard S., Handbook of Mathematical Tables and Formulas, 3rd Ed., Sandusky, Ohio: Handbook Publishers, Inc., 1954.

6. Laurson, Philip G., and Cox, William J., Mechanics of Materials, 3rd Ed., New York: John Wiley and Sons, Inc., 1954.

7. Streeter, Victor L., Fluid Mechanics, 2nd Ed., New York: McGraw-Hill Book Company, Inc., 1958.

8. Truxal, John G., ed., Control Engineer's Handbook, 1st Ed., New York: McGraw-Hill Book Company, Inc., 1958.

9. Partridge, Gordon R., Principles of Electronic Instruments, Englewood Cliffs, N.J.: Prentice-Hall, Inc., 1958.

VITA

Robert J. Beshara

Candidate for the Degree of

Master of Science

Thesis: THRUST-TIME MEASUREMENTS OF SMALL SOLID PROPELLENT ROCKET MOTORS

Major Field: Electrical Engineering

Biographical:

Personal Data: Born in Haskell, Oklahoma, October 5, 1931, the son of Thomas and Sally Mae Beshara.

Education: Graduated from Tahlequah High School, Tahlequah, Oklahoma, in May, 1949. Received Bachelor of Science at Oklahoma State University in January, 1958. Completed requirements for the Master of Science Degree at Oklahoma State University in May, 1961.

Military Experience: U. S. Navy, February, 1950 to November, 1953. Served as an aircraft electrician.

Professional Experience: Was employed by Douglas Aircraft Company, Inc., Tulsa, Oklahoma, as an Instrumentation Engineer from August, 1958 to April, 1960.

Professional Organizations: State Board of Registration for Professional Engineers (Oklahoma).